Additional Fire Exposure Time for the Effect of Spalling in Reinforced Concrete Columns

D. L. Peña (iD), *Civil Engineering Institute, Austral University of Chile, Valdivia, Chile*

C. Ibáñez (iD)*, *Concrete Science and Technology Institute (ICITECH), Universitat Politècnica de València, Valencia, Spain*

V. Albero (iD), *Department of Mechanical Engineering and Construction, Universitat Jaume I, Castellón, Spain*

A. Hospitaler (iD), *Concrete Science and Technology Institute (ICITECH), Universitat Politècnica de València, Valencia, Spain*

Abstract.   Concrete exposed to fire can experience spalling when the pore pressure increases due to water evaporation resulting in damage to part of the concrete cross-section which causes the loss of the initial cross-sectional symmetry, both thermal and geometrical. This may lead to what is, in essence, a biaxial bending problem in reinforced concrete columns. This study does not deal with the prediction of the occurrence of spalling for which a fully coupled hygro-thermo-mechanical analysis would be required. This work evaluates the consequences that corner spalling and surface spalling have on the fire resistance of reinforced concrete columns and presents a methodology based on the determination of a modified fire resistance time. An advanced fiber based numerical model for evaluating the fire resistance of RC sections exposed to fire is used as a tool to analyse the effect that spalling has on the performance of the columns. The model is able to generate the interaction surfaces of the columns subjected to uniaxial or biaxial bending and 4-sided exposed to the standard fire curve ISO 834. After a parametric analysis, it is observed that the negative effect of spalling can be quantified by means of an additional fire exposure time, which ranges between 0–35 min and depends on the column cross-section configuration, dimensions and load level. Finally, a proposal for the calculation of the modified fire resistance time for the effect of spalling is presented, which may be beneficial for practitioners in design.

List of Symbols

A_c	Concrete area
b	Square cross-section dimension
exp	Result obtained by experimental tests (subscript)
e_y	Y-axis eccentricity

---

*Correspondence should be addressed to: C. Ibáñez, E-mail: caribus@upv.es

e_z	Z-axis eccentricity
fiber	Result given by the numerical fiber model (subscript)
f_c	Concrete compressive strength
f_y	Yield strength of steel reinforcing bars
M_y	Applied bending moment in y-axis
M_z	Applied bending moment in z-axis
n_b	Number of reinforcing bars
N	Applied axial load
N_{max}	Maximum value of the cross-sectional resistance
pred	Result given by the proposal (subscript)
t	Required fire resistance time
t_{mod}	Modified fire resistance time
u_s	Reinforcement concrete cover
α	Neutral axis angle
ϕ	Bar diameter
κ	Curvature
λ	Slenderness ratio
ξ_{3D}	Three-dimensional error
μ	Load level
ω	Reinforcement ratio $(\omega = A_s f_y / A_c f_c)$

1. Introduction

Reinforced concrete (RC) exposed to fire can experience spalling when the internal pore pressure increases due to water evaporation, resulting in loss of concrete to a certain depth. Generally, spalling results in the loss of resistance of the cross-section of reinforced concrete elements. Parameters affecting the occurrence of spalling can be material related (concrete moisture content, concrete permeability and porosity, presence of cracks, concrete compressive strength, previous stress state, aggregate type and size, amount of reinforcement, or the concrete vibration technique adopted), geometry related (section shape and size, concrete cover and bars spacing), or ambient related (heating rate and regime, or loading conditions) [1–7].

The probability of spalling in different circumstances, as well as the causes producing it, are still up for debate and most of the current knowledge comes from the observation of the event on buildings and other structures exposed to fire. In these cases, the lack of instrumentation and reliable data results in primarily anecdotal conclusions being drawn. Provided that the proper conditions occur, any type of RC element can experience spalling, although, under identical conditions, it is difficult to predict which will spall. Spalling is a stochastic phenomenon that normally occurs within the first 30 min of fire exposure and can affect any area of the exposed RC element. Although different approaches and classifications can be found in the literature, the range of time occurrence seems to be relatively well established for the worst case scenarios in which the reduction of the effective cross-section can have serious consequences on the fire resistance of RC elements ([1–3, 8]). Along a similar vein, spalling has been observed fairly regularly with depths up to 45 mm occurring in one stage, or several stages, with layers ranging from 15 to 20 mm in depth [8]. The worst case scenario however has been identified to be when spalling results in the complete loss of concrete cover, directly exposing the reinforcement to the heat source [3].

Experimental programs on reinforced concrete sensitivity to spalling can be performed on small, medium or full-scale tests, either on loaded or unloaded conditions. In small-scale investigations, temperature and pressure are usually monitored in unloaded prismatic RC specimens. This is the case of the small-scale research conducted by Lo Monte and Gambarova [9] which focused on corner spalling, where the thermal dilation along two converging planes was found to be the dominant fracture mechanism. Medium-scale tests normally consist in slabs or prismatic specimens heated on one side, again either loaded or unloaded. From small and medium scale tests results common conclusions can be drawn: (1) spalling sensitivity increases from unloaded to loaded conditions; and (2) biaxial compression is a more severe condition than uniaxial loading [10].

Lastly, full scale researches comprise testing structural members or substructures under restraining and loading conditions characteristic of the real ones. Although this experimental level is, evidently, the most representative of the actual structural behaviour, it is expensive and time demanding [11]. Along these lines and specifically regarding RC columns, Buch and Sharma [12] pointed out in a recent paper the importance of studying the fire resistance of structures subjected to eccentric loads combined with spalling. After performing a series of experiments, it was observed that load eccentricity increases the occurrence of spalling. As with Khoury [2], they proved the effectiveness of reinforcing bars in limiting spalling, particularly if these are distributed along the sides of the cross-section.

Some researchers have developed models focused on predicting the occurrence of spalling. Dwaikat and Kodur [13] developed a one-dimensional model based on pore pressure calculation. Lottman et al. [14] presented a model based on two coupled finite elements models where the first one finds the temperature and pore pressure evolution and the second defines the fracture mechanism causing spalling. However, given the stochastic nature of the phenomenon it is not easy to draw solid conclusions about this.

On the contrary, the work presented in this paper does not deal with modelling the mechanism or the time to occurrence of spalling. It is instead assumed that spalling occurs, and the effects that this phenomenon has on the performance of the columns are analysed after the fact.

When spalling occurs, the loss of part of the concrete cross-section (e.g., concrete cover) leads to the loss of the initial cross-sectional symmetry, both thermal and geometrical. This non-symmetrical geometry may lead to what is, in essence, a biaxial bending problem. The core and reinforcing bars may become exposed to fire after the loss of part of the concrete cover. This may lead to a rapid increase in temperature and a reduction in the fire resistance of the column, resulting in a decrease in the level of safety of the column when designed using the prevailing fire resistance design framework [7].

This paper presents a study into the effects of spalling on reinforced concrete columns when it affects either the corner of a column or the surface of one of the sides. Subsequently, a methodology based on the determination of a modified fire resistance time for the effect of spalling in reinforced concrete columns is proposed. To this end, an advanced fiber-based numerical model previously developed by the authors for evaluating the fire resistance of RC columns exposed to

fire is described in this paper. The model is able to obtain the cross-sectional interaction diagrams in 2D or 3D (Sect. 2.1). For the determination of the temperature field of the section at elevated temperatures the finite difference method is used. The fiber model validation (Sects. 2.2 and 2.3) against experimental and numerical data for RC columns is described.

Next, the fiber model is applied for the evaluation of the effect of corner and surface spalling on the fire resistance of RC columns (Sect. 3) and after a detailed description, two cases of study are presented.

In turn, a parametric study is developed (Sect. 4.1) using the advanced fiber numerical model to consider the effect of different parameters on the severity of the consequences of spalling. The parametric analysis also allows for the comparison of the effects of surface and corner spalling. Finally, this is used to build the proposal to calculate a modified fire resistance time for the effect of spalling in reinforced concrete columns which may be beneficial for practitioners in design (Sect. 4.2).

2. Model Description and Validation

In this section, the description and validation of a fiber numerical model developed by the authors are summarised. The model was presented by the authors in a previous publication [15] and in this paper it is applied for the evaluation of the effect of spalling. In fact, the aim of this work is to propose a methodology to evaluate the effect of spalling on the fire behaviour of RC columns when it is necessary to consider its occurrence.

For a real building, the common loading situations for reinforced concrete (RC) columns may be compression combined with biaxial bending due to the load transferred from adjacent beams and slabs. This loading condition also appears when a RC column is non-uniformly exposed to fire because the sectional temperature field becomes non-symmetric, which also happens when spalling occurs (Fig. 1). Under these circumstances, the procedure to obtain the fire resistance of the RC section becomes more difficult as the number of investigations found in literature about the fire design of RC columns under these loading conditions is limited [15]. With regard to this, the works by Wang et al. [16] and Kodur and Raut [17] must be highlighted. In these works, RC columns non-symmetrically exposed to fire were numerically studied. Wang et al. [16] assessed the applicability in the fire situation of the ambient temperature method proposed in EN 1992-1-1 [18] through a previously experimentally validated model and defined the powers of the non-dimensional interaction equation as a function of different parameters. Kodur and Raut [17] performed a numerical study on the fire capacity of RC columns under biaxial bending and evaluated the influence of non-symmetric fire exposures and spalling. With the results of a parametric analysis, an equation was proposed and validated with experimental data.

It is noteworthy that EN 1992-1-2 [19] provides specific actions to prevent it from happening in the case of high strength concrete. But when spalling cannot be avoided, EN 1992-1-2 [19] Clause 4.1(2) indicates that the influence of spalling on
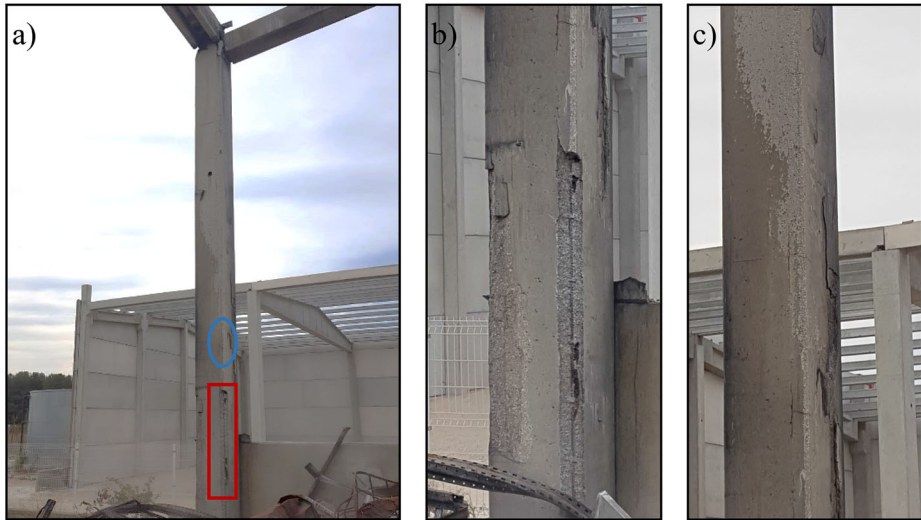
Figure 1. (a) RC Column at Industrial Building After a Fire; (b) and (c) Detail of Corner and Surface Spalling in the RC Column.

the performance requirements shall be taken into account. However, it does not include any specific design model that considers the effect of spalling on the cross-section fire resistance of RC columns.

Taking this into consideration, in this paper a sectional model for the effect of spalling on the fire resistance of RC columns exposed to fire is described. The model focuses on the cross-sectional mechanical behaviour at high temperatures. Therefore, second order effects and buckling behaviour have not been considered in this analysis.

2.1. Numerical Fiber Model Description

The model presented in this work is a sectional model with fiber integration (Fig. 2a) developed in MATLAB [20]. A sequentially coupled thermal-stress analysis is conducted: firstly, a thermal analysis (by finite differences) is carried out, and then the mechanical problem is solved.

The values recommended in EN 1991-1-2 [21] are used for the main heat transfer parameters. Through mechanisms of convection and radiation, the standard temperature–time curve is applied to the exposed surface.

The cross-section is discretised (Fig. 2a) and each cell is characterised by its position, its temperature, and its corresponding material properties. In this case, for both reinforcing steel bars and concrete, the thermal and mechanical properties given by EN 1992-1-2 [19] are used. The effects of transient creep strains are implicitly considered by the EN 1992-1-2 [19] concrete material model. When not specified in the literature, siliceous aggregates are considered. Since tensile strength of concrete is generally considered negligible, in this model it is neglected which is on the safe side for design purposes. Also perfect bond is assumed in the analysis
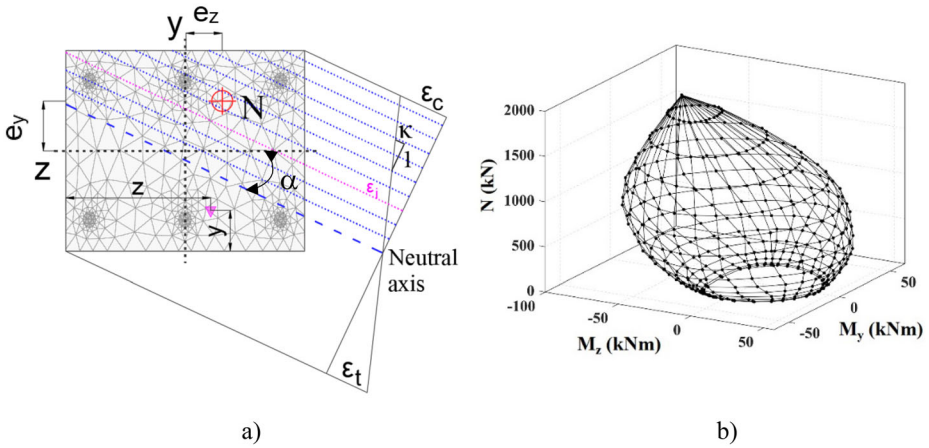
Figure 2. Fiber Model (a) Cross-Section Discretization and Strain Distribution; (b) 3D Failure Surface.

as usually is done for RC concrete structures, implying full compatibility between concrete and reinforcement strains.

For the analysis, the Navier-Bernoulli assumption is adopted, which states that a plane section remains plane and normal to the neutral axis (Fig. 2a) after bending. Therefore, the curvature of the cross-section (κ) can be derived from the linear distribution of total strains. In this work, mechanical strains are equal to total strains minus thermal strains.

The stress state of each cell is obtained from the constitutive equation of the material at the corresponding temperature. For a given applied axial load N and through an iterative process, the location of the neutral axis is determined based on the force balance equation that is presented in Eq. (1).

$$\sum_{i=1}^{n} A_i \sigma_i - N = 0 \tag{1}$$

where A_i is the area of cell i (mm^2), σ_i is the stress of cell i (N/mm^2),
N is the axial load applied (N).

The bending capacity in each axis is determined by solving Eqs. (2) and (3) by gradually increasing the value of the curvature of the cross-section in order to generate the M-κ curve.

$$\sum_{i=1}^{n} A_i \sigma_i z_i - M_y = 0 \tag{2}$$

$$\sum_{i=1}^{n} A_i \sigma_i y_i - M_z = 0 \tag{3}$$

where y_i is the y-axis position of the centroid of cell i (mm),z_i is the z-axis position of the centroid of cell i (mm),

M_y is the applied bending moment in y-axis (Nmm),

M_z is the applied bending moment in z-axis (Nmm).

To obtain the interaction surface, the balance equations are solved for all the loading situations generated by rotating the neutral axis (angle α in Fig. 2a), and increasing the axial load from 0 up to the value of the cross-sectional plastic resistance (N_{max}). In the example of Fig. 2b, an interaction surface generated by means of the described fiber model for a RC column with 3-sides exposed to the ISO 834 [21] fire standard curve is shown. It is necessary to get the M-κ diagram for each point in order to calculate the points of the failure surface.

2.2. Thermal Validation

The thermal model was validated with the experimental temperatures recorded in the tests carried out by Lie and Irwin [22] and Kodur et al. [23]. In the validation, the predictions given by the model for the inner points of the concrete cross-section at different fire exposure times were compared with experimental values. To illustrate this process, in Fig. 3 it is shown the validation for one of the columns with square cross-section of 305 × 305 mm, 4 reinforcing bars of diameter 8 mm,
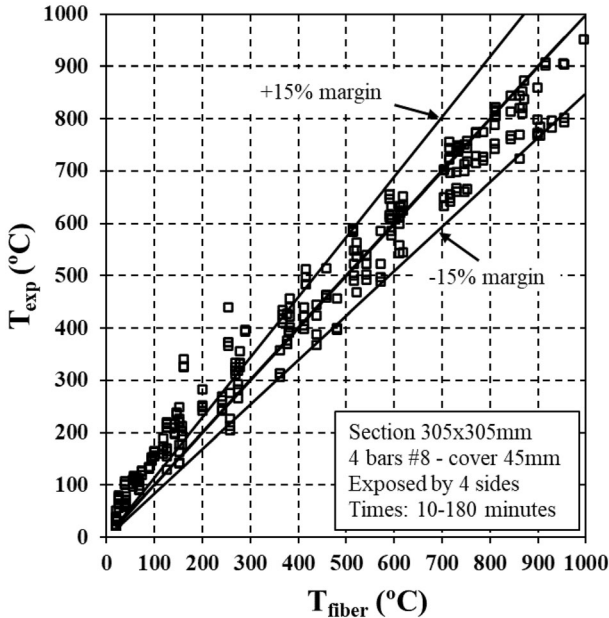

Figure 3. Tests vs. Predictions. Col. 1 Lie and Irwin [22].

a concrete cover of 45 mm, and exposed on four sides to a standard heating for 180 min (Col.1 from [22]). It can be clearly observed that the points lie mainly in the inner part of the ± 15% boundaries and that the precision of the model increases for temperatures higher than 400°C. As an example, the predicted temperature–time curves at the location of two of the thermocouples placed at the cross-section are plotted against the experimental points in Fig. 4. As seen, the model predicts with good accuracy the evolution of the temperatures along time. More details about the specimens used in validation can be found in [15].

2.3. Mechanical Validation

Given the lack of experiments on columns subjected to biaxial bending in fire, the validation of the mechanical model is completed by parts: (1) validation at ambient temperature for biaxial bending and (2) validation at high temperatures under uniaxial bending. For the ambient temperature validation, experimental results from different published works [24, 25] were used. In total 41 specimens were selected as summarised in Table 1. Note that according to EN 1992-1-1 [18] Clause 5.8.3.1, second order effects may be ignored if the slenderness ratio (λ) is below a certain limit ratio value (λ_{lim}). This limit ratio is calculated and shown in Table 1. As can be observed, the specimens' slenderness ratio values are below the limit or very close to it. Therefore, the second order effects in these columns can be neglected. Figure 5 shows the good agreement that exists between tests and predicted results for the 41 cases used in validation (Mean = 0.98, SD = 0.20).

For the validation at high temperatures under uniaxial bending, the model predictions have been validated against those presented by Law and Gillie [26]. The specimen taken as reference (300 × 500 mm, 6ϕ20) is a ISO 834 standard fire curve [21] 3-sided exposed reinforced concrete column. The predictions given by both models are identical as can be seen in Fig. 6.
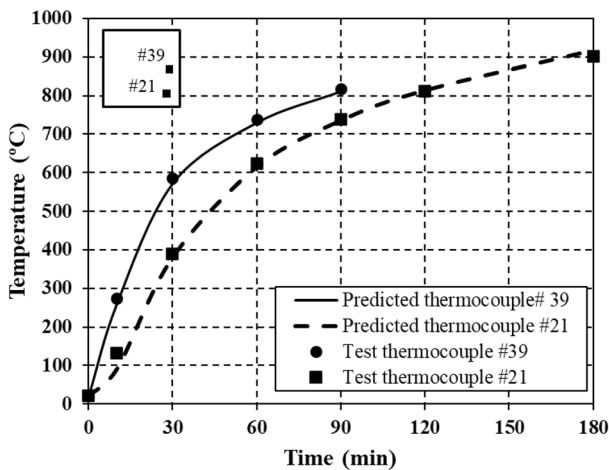

Figure 4. Predicted Temperatures. Col. 1 Lie and Irwin [22].

Table 1
Details of Specimens Used in Validation for Biaxial Bending at Ambient Temperature

| Ref	ID	f_c (MPa)	f_y (MPa)	ω	λ	λ_{lim}	N_{exp} (kN)	N_{fiber} (kN)	ξ_{3D}
Bresler [24]	B-1	25.5	368.9	0.37	21	32.2	106.8	110.1	0.97
	B-2	26.9	368.9	0.35	21	29.4	266.9	283.6	0.94
	B-3	25.5	368.9	0.37	21	46.4	311.4	313.1	0.99
	B-4	31.7	368.9	0.30	21	41.8	142.3	132.1	1.08
	B-5	22.1	368.9	0.43	21	59.6	142.3	155.0	0.92
	B-6	25.5	368.9	0.37	21	52.7	75.6	77.8	0.97
	B-7	24.1	368.9	0.39	21	49.7	93.4	99.1	0.94
	B-8	24.8	368.9	0.38	21	41.1	106.8	104.9	1.02
Ramamurthy [25]	A-4	47.9	234.4	0.12	34	43.3	283.6	229.2	1.24
	A-5	42.7	234.4	0.14	34	49.2	235.8	179.3	1.32
	A-6	40.3	234.4	0.14	34	27.1	171.9	141.4	1.22
	A-8	31.9	234.4	0.18	34	40.6	475.6	506.0	0.94
	A-9	46.2	234.4	0.12	34	54.0	280.24	217.8	1.29
	A-12	49.6	234.4	0.12	34	40.0	170.14	161.0	1.06
	A-13	20.9	234.4	0.28	34	45.4	164.58	138.7	1.19
	A-14	29.6	234.4	0.19	34	32.6	160.1	118.8	1.35
	A-15	23.7	234.4	0.24	34	27.1	266.9	231.1	1.16
	B-1	32.4	322.6	0.38	34	23.6	628.98	669.6	0.94
	B-2	28.6	322.6	0.43	34	30.6	771.8	853.5	0.90
	B-3	37.2	322.6	0.33	34	35.1	533.8	556.4	0.96
	B-4	35.6	322.6	0.35	34	30.0	395.9	426.6	0.93
	B-6	30.6	322.6	0.41	34	30.0	500.4	550.0	0.91
	B-7	32.7	322.6	0.38	34	37.1	516.0	509.2	1.01
	B-8	37.9	322.6	0.33	34	19.3	369.8	370.9	1.00
	D-1	35.1	322.6	0.42	31	23.8	785.1	881.3	0.89
	D-2	28.2	322.6	0.39	35	28.8	400.3	414.0	0.97
	D-3	27.1	322.6	0.55	31	19.6	311.4	298.4	1.04
	D-4	27.9	322.6	0.53	31	33.9	680.6	729.4	0.93
	D-5	34.3	322.6	0.43	31	30.9	378.1	367.1	1.03
	D-6	26.5	322.6	0.56	31	26.6	400.3	386.5	1.04
	E-1	26	322.6	0.43	23	31.7	464.8	462.2	1.01
	E-2	23.8	322.6	0.47	23	28.7	311.4	340.3	0.92
	E-3	30.8	322.6	0.36	23	24.9	435.9	411.2	1.06
	E-4	27.6	322.6	0.40	23	27.3	542.7	566.2	0.96
	F-1	32.5	291.9	0.26	31	29.6	600.5	692.7	0.87
	F-3	20	291.9	0.43	31	30.1	384.8	441.0	0.87
	F-5	29.6	291.9	0.29	31	23.2	466.0	537.9	0.87
	G-1	36.6	291.9	0.17	23	25.8	827.4	899.0	0.92
	G-2	28	291.9	0.23	23	22.3	418.1	460.5	0.91
	G-3	24	291.9	0.27	23	33.1	507.1	574.7	0.88
	G-4	41.4	291.9	0.15	23	32.2	333.6	356.3	0.94
								Mean	0.98
								SD	0.20
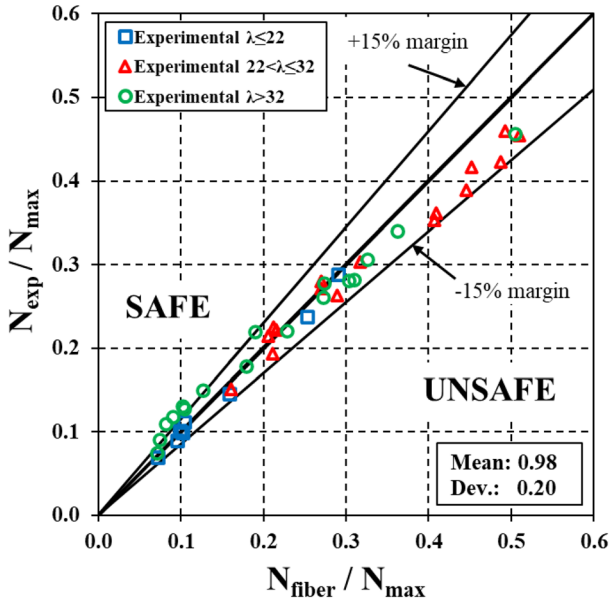
Figure 5. Experimental vs. Fiber Model Predictions.

3. Application of the Model for the Evaluation of the Effect of Spalling

3.1. Study Description

In this section, the model described is applied to evaluate the effect of corner and surface spalling in RC columns. The times to the occurrence of spalling and the depth of spalling are set based on the conclusions obtained after the analysis of the reviewed literature.

As discussed in Sect. 1, the worst case scenario has been identified to be when spalling results in the complete loss of concrete cover, directly exposing the affected reinforcement to the heat source [3]. In addition, according to EN 1992-1-2 [19], in those cases where the influence of spalling on the load-bearing capacity of a structural element has to be assessed, it will be done by assuming local loss of cover to one reinforcing bar or bundle of bars in the cross section and then checking the reduced load-bearing capacity of the section. For this verification the temperature of the other reinforcing bars may be assumed to be that in an unspalled section.

Therefore, in this study for both corner and surface spalling the local loss of the concrete cover is assumed. The geometry of the damage is set so that half of the perimeter of the affected reinforcing bar is directly exposed to fire (see corner bar in Fig. 7a and side bar in Fig. 7b), as this assumption is conservative. As can be seen in Fig. 7a and Fig. 7b, the geometry of the spalled area varies between corner and surface spalling respectively.
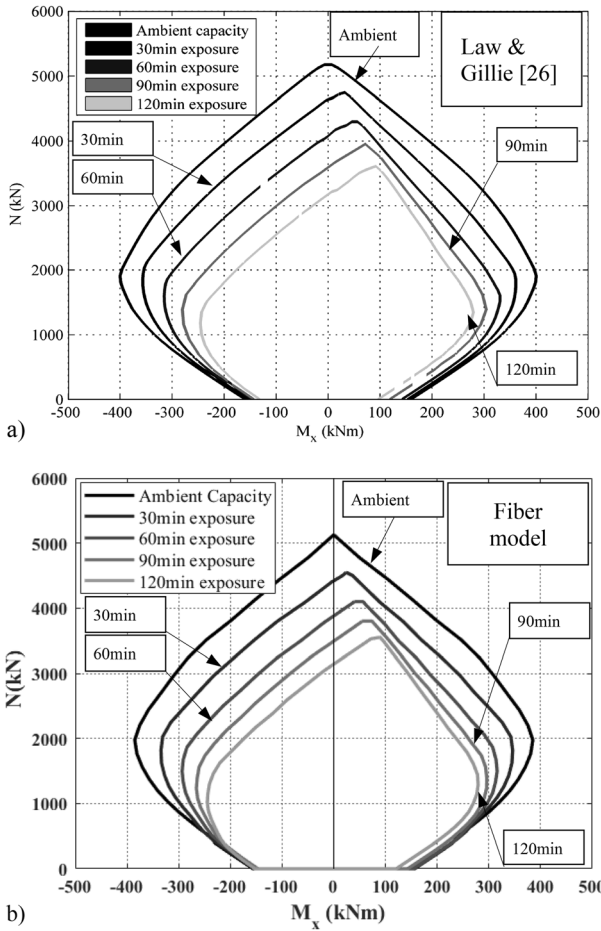
Figure 6. Uniaxial Interaction Diagrams for Different Required Fire Resistance Times.

In order to illustrate the procedure followed, a square RC column exposed on four sides to the ISO 834 standard fire curve [21] is considered. A cross-section measuring 300×300 mm with $8\phi16$ reinforcing bars and a concrete cover of 35 mm is taken as reference for the study developed. A concrete compressive strength of C30 and a reinforcing bars yield strength of $f_y = 500$ MPa are adopted for the RC column.

First, the evolution in time of the cross-sectional temperatures is obtained and, when spalling occurs, its effect is evaluated by eliminating the fibers of concrete affected (Fig. 7a and b). This leads to the loss of the initial cross-sectional symmetry, both thermal and geometrical. Therefore, the cross-sectional temperatures must be updated for the new boundary conditions, as shown in Fig. 8b and c for
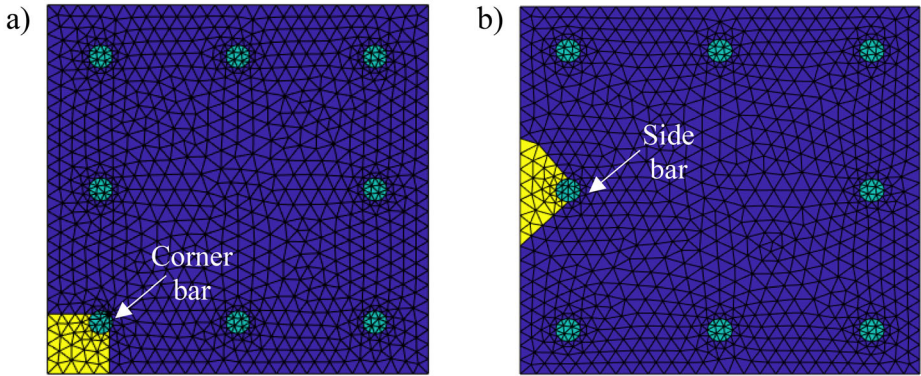
Figure 7. (a) Corner Spalling Modelling; (b) Surface Spalling Modelling.
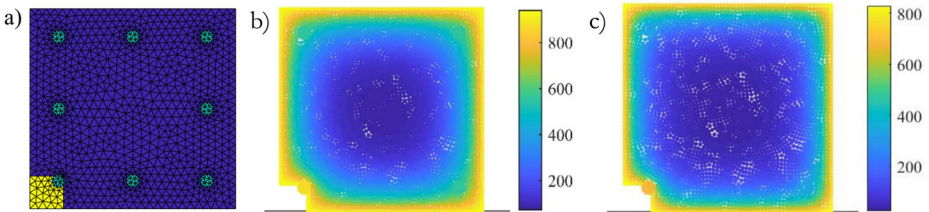
Figure 8. (a) Corner Spalling Modelling; (b) Temperatures at 60 min; (c) Temperatures at 90 min.

the case of corner spalling. This non-symmetrical geometry leads to what is, in essence, a biaxial bending problem.

The preliminary study begins with the analysis of the influence of the time of spalling occurrence. According to the literature revisited, the times considered are 10, 20 and 30 min from the start of heating. Figure 9 shows a detail of the area affected by spalling where the numbers 1 to 3 correspond to the points where the temperature is measured for the following study: point 1 represents the temperature at the exposed reinforcing bar; and point 2 and 3 correspond to the concrete temperature around the spalled area.

For the reinforcing bar that is left directly exposed to fire after corner spalling (point 1), Fig. 10a shows the evolution of the temperature for the different times of spalling occurrence. For surface spalling, Fig. 11a displays the evolution of the temperature in the reinforcing bar (point 1). In varying the time of spalling it is observed that the importance of this parameter decreases as the exposure time increases. For fire exposure times higher than 45 min, the time of spalling has no remarkable effect. As a reference, the concrete temperatures around the spalled area for two points (point 2 and point 3) are displayed in Fig. 10b and c for corner spalling, and in Fig. 11b and c for surface spalling. As expected, given the lower conductivity of concrete, after 45 min of fire exposure, the temperature in
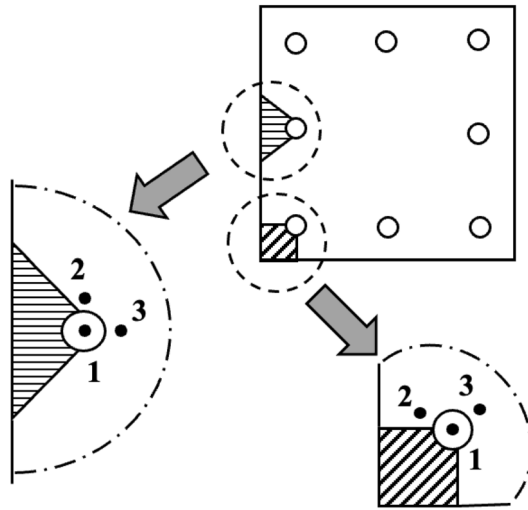
Figure 9. Details of Spalling Area.

case of spalling occurring at 30 min is a slightly lower than for the other two, but the difference is small enough to draw the same conclusion.

Regarding concrete temperature through the cross-section, the same analysis can be done from Figs. 12 and 13 where the histories of temperatures for three representative points of the cross-section are shown. As expected, the effect of the spalling area is more notable for point B/6 than for points B/4 and B/2. In all the cases, the effect of the time of spalling occurrence is less important for higher fire exposure times. This highlights that, at least for the cases of reference, the time of spalling occurrence has no influence unless the fire resistance behaviour is evaluated for a fire exposure time less than 45 min.

A similar approach was followed by Dotreppe et al. [1] which also considered that the effect of spalling became stable from 30 min on. However, in this case, the authors progressively reduced the effective cross-section due to spalling effect during the first 30 min of heating, instead of considering a certain spalling initiation time with an associated degree of damage.

In any case, in terms of fire resistance, spalling becomes significant due to the consequent reduction in the concrete cover causing the reinforcing steel to be directly exposed and heated more rapidly, leading to premature loss of overall structural capacity. The area of the cross-section affected is usually not large enough to alter the transmission of heat through the unspalled concrete of the cross-section.

3.2. Corner Spalling

For corner spalling, in Fig. 8b and c, the cross-sectional temperatures for 60 and 90 min of fire exposure are shown. The temperature in the corner reinforcing bar
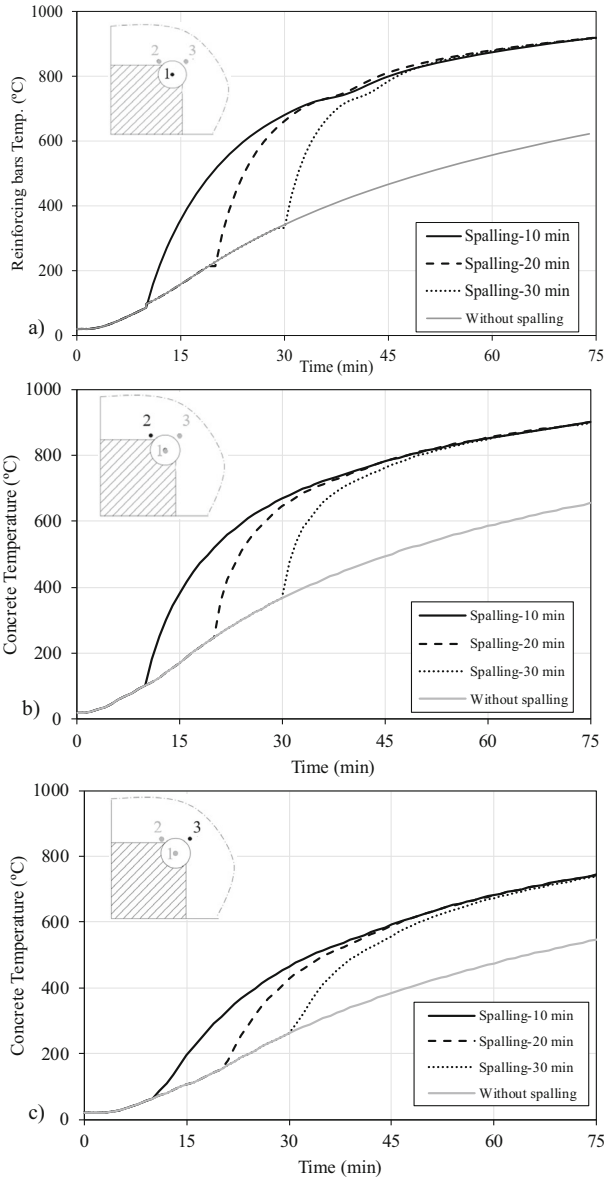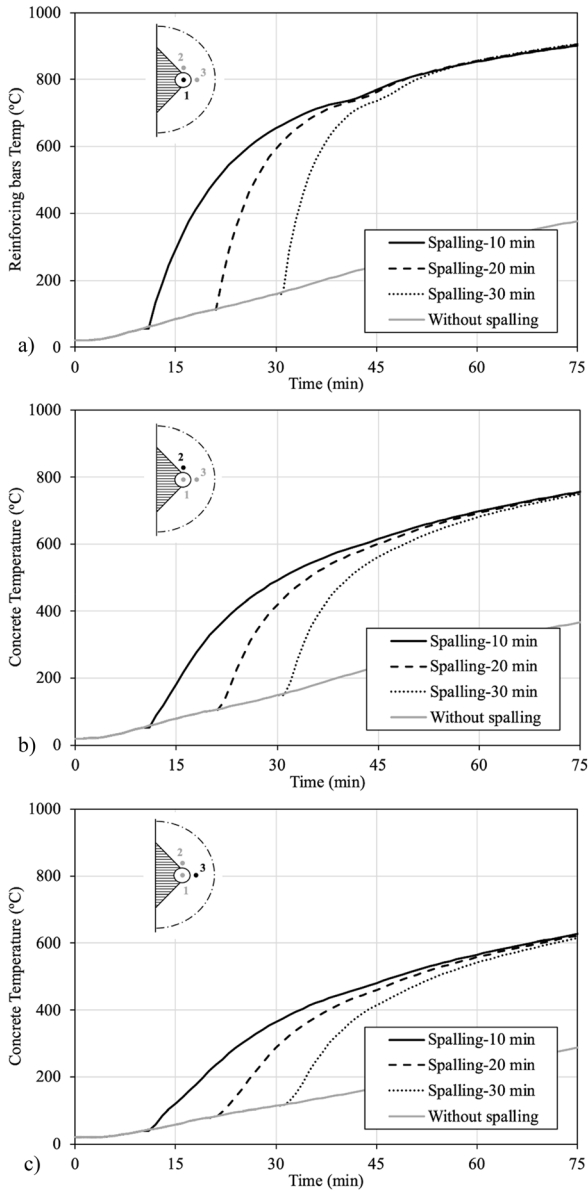
Figure 10. Temperatures at the Area Affected by Corner Spalling: (a) Reinforcing Bar Point 1; (b) Concrete Point 2; (c) Concrete Point 3.

that now is exposed directly to fire is much higher than the other bars as expected.

As explained in the previous section, the time of spalling occurrence has no influence for fire resistance times higher than 45 min. This observation is corroborated by the mechanical response given by model and shown in Fig. 14. In this

Figure 11. Temperatures at the Area Affected by Surface Spalling: (a) Reinforcing Bar Point 1; (b) Concrete Point 2; (c) Concrete Point 3.

figure several interaction surfaces for columns exposed for 60 min with different spalling times are shown, and it can be seen that they are identical. This is likely a result of the fact that, after 60 min of exposure, the temperature of the concrete on the surface has surpassed the point of being structurally viable and does not
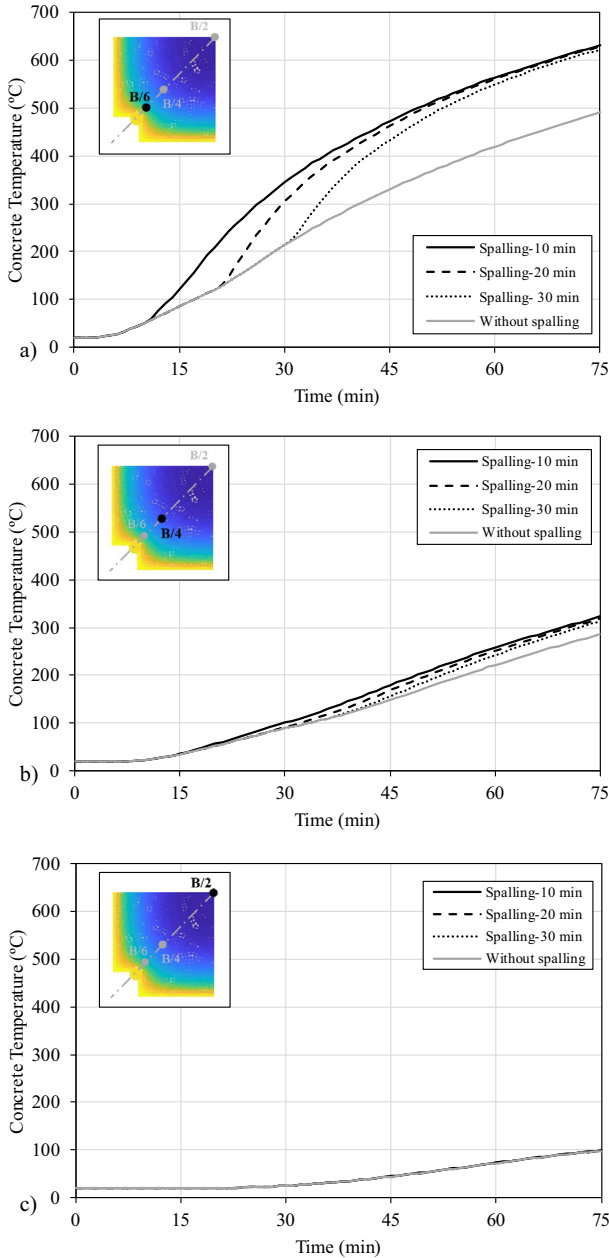
Figure 12. Corner Spalling—Concrete Temperatures at: (a) Center B/2; (b) B/4; (c) B/6.

therefore contribute to the performance of the column. The temperature gradient within the column is the dominating factor (in this specific spalling scenario) in the performance of the column.
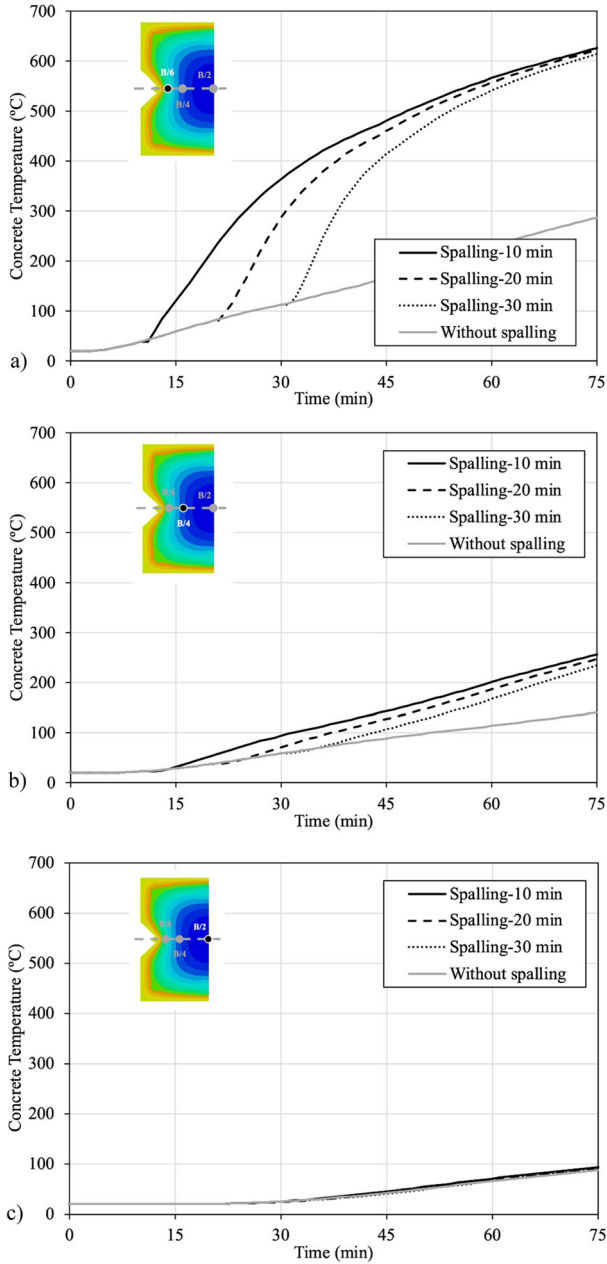
Figure 13. Surface Spalling—Concrete Temperatures at: (a) Center B/2; (b) B/4; (c) B/6.
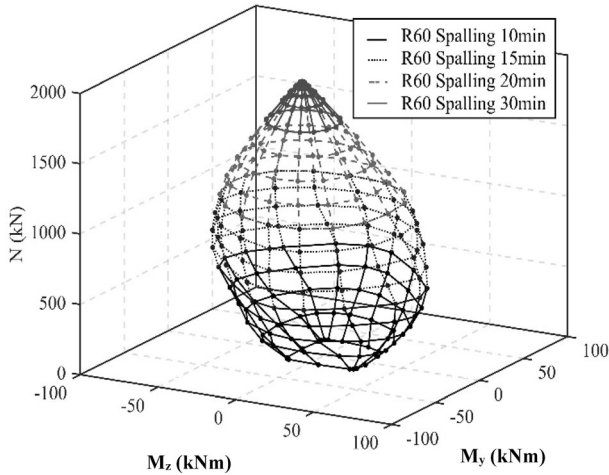
Figure 14. Superposition of Interaction Surfaces for 60 min of Fire Exposure.

From the interaction surfaces, the M_y-M_z interaction diagrams for certain load ratios can be obtained by taking slices. Thus, for the same load ratio, it is possible to compare diagrams of columns with and without spalling. The decrease in the fire resistance due to spalling can be quantified by finding the diagram modelled without spalling that, in the most critical quadrant, coincides with the diagram modelled with spalling.

In Fig. 15 the 90-min interaction diagram for a RC cross-section where spalling has occurred is shown with a dotted line. This diagram is obtained by taking a slice of the 3D interaction surface at the plane of the axial load corresponding to a load level of 0.4 (750 kN). Note that, as explained above, the spalling produces an asymmetry in the interaction diagram. In the same graph of Fig. 15, with a continuous line, the diagram for the same section without spalling, for the same load level and a fire exposure of 100 min is shown. It can be observed that, since spalling has not appeared, in this case the diagram is symmetric.

As can be seen, in the first quadrant both diagrams coincide in the most critical part of the 90-min diagram (with spalling). This means that the most serious situation for a required fire resistance time of 90 min with spalling is equivalent to the situation where the RC cross-section has a fire resistance time of 100 min without spalling. Herein this will be referred to as modified fire resistance time (Eq. 4). Therefore, the effect of spalling in a cross-section implies an additional fire exposure time (AFET) which means extending the heating of the cross-section for an extra time (another 10 min in this case) but without spalling occurrence.
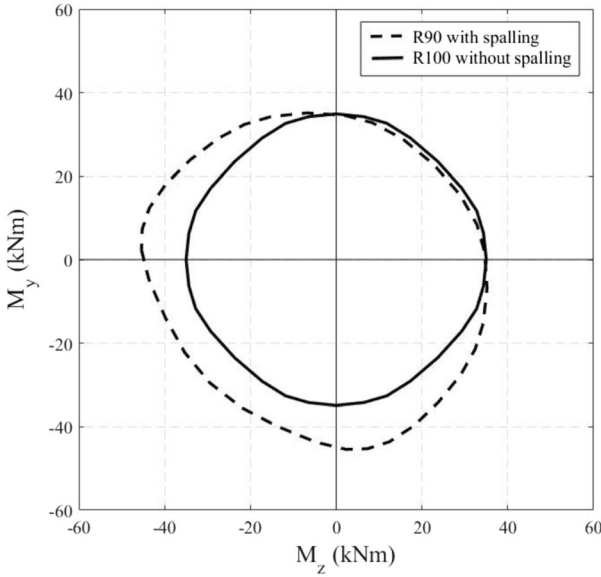
$$t_{mod,fiber} = t + AFET \tag{4}$$

Figure 15. Corner Spalling: 90-min Interaction Diagram μ=0.4.

where $t_{mod,fiber}$ is the modified fire resistance time in min given by the numerical fiber model, t is the required fire resistance time in min, and AFET is the additional fire exposure time in min given by the numerical fiber model.

3.3. Surface Spalling

The same procedure is followed to study the effect of surface spalling in the fire resistance of the section of reference. In the same way, in Fig. 16 the dashed line represents the 90-min interaction diagram for a RC cross-section where spalling has occurred, taken at the plane of the axial load corresponding to a load level of 0.4. The continuous line stands for the diagram for the same section without spalling, for the same load level and a modified fire resistance time of 120 min. It can be observed that, in this case, in the most critical point, both diagrams match. This means that the occurrence of spalling involves an AFET of 30 min, equivalent to extending the fire exposure of a section without spalling for that additional time.

In this preliminary analysis, considering the results of Figs. 15 and 16, it can be observed that surface spalling has worse consequences and a more negative effect on the fire resistance of the RC column since considering its occurrence is equivalent to applying an AFET much higher (30 min) than in the case of corner spalling (10 min). In order to compare the effect of both types of spalling in the fire resistance time of RC columns, and to assess the AFET for other column configurations, a parametric analysis is carried out and presented in the next section.
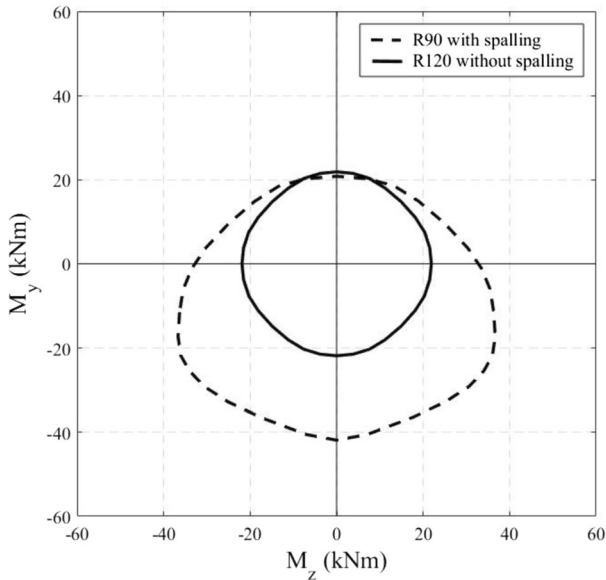
Figure 16. Surface Spalling: 90-min Interaction Diagram μ=0.4.

4. Parametric Analysis

The different effect of corner and surface spalling on the modified fire resistance time is evaluated in this section by means of a parametric study where both types of spalling are considered. The parameters taken into account in the analysis are: the cross-section dimensions, the concrete cover, the load level, the number of reinforcing bars and their diameter, and the required fire resistance time. In Table 2, the values adopted for the different parameters are shown. In total 324 different column configurations for corner spalling are considered. Additionally, 162 cases were modelled for surface spalling, because only the configuration with

Table 2
List of Parameters

Parameters	Values
Type of spalling	Corner (Fig. 7a); Surface(Fig. 7b)
Spalling initiation time (min)	15
Square cross-section dimension [b] (mm)	250; 300; 400
Concrete cover [u_s] (mm)	30; 35; 40
Load level [$\mu = N/b^2 f_c$]	0.2; 0.4; 0.6
Number of reinforcing bars [n_b]	4; 8
Bar diameter [Ø] (mm)	12; 16; 20
Fire resistance time [t] (min)	60; 90; 120

n_b = 8 reinforcing bars is considered. Note that the spalling initiation time is set to 15 min for all of the cases since it has proven not to have a remarkable effect for the fire resistance times considered.

Again, for both corner and surface spalling, the local loss of the concrete cover is assumed following the guidelines by EN 1992-1-2 [19] for the worst case scenario. As described above, the geometry of the damage is set so that half of the perimeter of the affected reinforcing bar is directly exposed to the heat source. Considering all the sections from Table 2, this assumption leads to spalling areas ranging from 0.7 to 3.4% of the cross-section for corner spalling and ranging from 0.8 to 3.2% in the case of surface spalling. These percentages are minimal so it is assured that the area affected is not large enough to influence the heat transmission through the non-affected concrete of the cross-section.

Subsequently, the aim of this study is to elaborate expressions for the prediction of the modified fire resistance time that may be useful for practitioners in their daily practice. The proposal is the result of a curve fitting procedure made from numerical results given by the fiber model developed by the authors and presented in the Sect. 2.

4.1. Results from the Parametric Analysis

In Fig. 17 the different values of the AFET obtained with the fiber model for the cases considered in the parametric are shown. As can be seen, the dots in red correspond to the corner spalling cases, whereas the black dots represent the surface spalling cases. In these graphs, only the cases with n_b = 8 reinforcing bars are shown for sake of comparison.

As can be observed, the effect of surface spalling on RC columns is generally more serious than the effect of corner spalling, as the values of the AFET are higher. This corroborates the preliminary result commented in Sect. 3. This can be due to the fact that in RC columns with 8 reinforcing bars, those placed at the corners suffer a quicker degradation, even without the occurrence of spalling, since they are affected by bidirectional heating (corner bar in Fig. 7a). The reinforcing bars on the sides affected by surface spalling (side bar in Fig. 7b) degrade slower, so the loss of resistance that they experience due to spalling has a more remarkable effect on the fire resistance of the RC column, as they are left directly exposed to the heat source.

It can be seen that there is no profound difference in the effect of the two types of spalling for a required fire resistance time of R60 and high values of concrete cover, where the temperature of corner and side reinforcing bars are similar due to the protection provided by the concrete cover. The overall trend observed in Fig. 17 suggests that, as the required fire resistance time increases and the concrete cover decreases, the effect of each type of spalling can be more clearly differentiated.

Following a conservative approach, only surface spalling, which produces higher loss of cross-sectional strength, should be considered in design for RC columns with 8 reinforcing bars and fire resistance requirements equal or higher than 90 min. On the contrary, in RC columns with fire resistance requirements lower
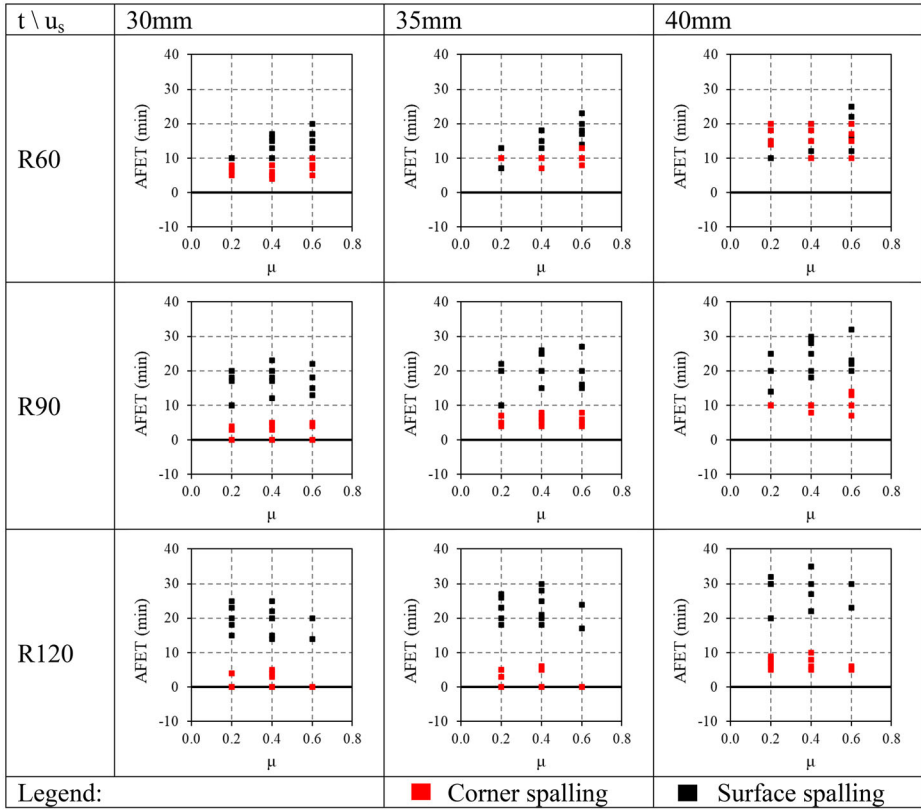
Figure 17. Additional Fire Exposure Times (AFET) for Corner and Surface Spalling.

than 90 min, both corner and surface spalling should be taken into account in design in order to assess which one is more damaging. For RC columns with 4 reinforcing bars, just corner spalling should be explicitly considered.

4.2. Proposal for the Modified Fire Resistance Time for the Effect of Spalling

In this section the expressions proposed for the authors for the modified fire resistance time for the effect of spalling in RC columns are presented. The expressions have been developed for corner and surface spalling respectively.

The proposal is the result of a curve fitting procedure developed from the results obtained by the fiber model presented. First, the results of the parametric analysis were statistically assessed in order to obtain the influence of each parameter in the modified fire resistance time. Then, a multi-variant approach was performed in order to obtain the weight coefficient for each parameter. The expressions resulting from this procedure may be helpful for practitioners when

designing RC columns and considering the effect of spalling on the evaluation of their fire resistance times.

Corner Spalling In the case of corner spalling, Eq. (5) shows the expression proposed:

$$t_{\text{mod},pred} = 0.92t + 0.81u_s - 1.46n_b \tag{5}$$

where $t_{mod,pred}$ is the modified fire resistance time in min predicted by the equation, t is the required fire resistance time in min, u_s is the concrete cover in mm, and n_b is the number of reinforcing bars along the cross-section.

In Fig. 18a, the comparison of the predicted modified fire resistance times ($t_{mod,pred}$) with the values obtained by the fiber numerical model ($t_{mod,fiber}$) is plotted. As can be seen all of the points lie in the inner part of the $\pm$ 10% boundaries and most of them are mainly placed on the safe side. The error is calculated as the ratio between the modified fire resistance time predicted by the equation and the modified fire resistance time given by the numerical fiber model: $t_{\text{mod},pred}/t_{mod,fiber}$ so a value higher than 1 means that the equation proposed is conservative. In this case, the mean of the error is 1.03 and the standard deviation is 0.03, which shows a good agreement of the predicted values with those given by the fiber model.

Surface Spalling On the other hand, the proposal for the calculation of the modified fire resistance time for surface spalling is shown in Eq. (6):

$$t_{\text{mod},pred} = 1.17t + 0.58u_s + 12.00\mu - 0.05b - 4.00 \tag{6}$$

where $t_{mod,pred}$ is the modified fire resistance time in min predicted by the equation, t is the required fire resistance time in min, u_s is the concrete cover in mm, μ is the load level defined as $\mu = N/b^2f_c$, and b is the square column dimension in mm.

Again, the predicted values are compared with those given by the fiber model as displayed in Fig. 18b where it is observed that, again, all of the points lie in the $\pm$ 10% boundaries, mainly on the safe side. For surface spalling, the mean of the error is 1.01 and the standard deviation 0.03, values that prove that the proposal is able to predict the modified fire resistance time with accuracy.

In turn, it is important to notice that the applicability of the equations proposed above is limited to the ranges set by the values defined in Table 2, and that they are based on the specific type of occurrence of spalling adopted in this work (Fig. 7). This proposal provides a way to quantify the effect of spalling on the cross-sectional fire resistance of RC columns by means of a modified fire resistance time. Given the lack of solid experimental evidence, some key assumptions were made that should be considered when applying the proposal. The second order effects and buckling behaviour have not been considered in this analysis that focused on the cross-section mechanical behaviour at high temperatures. Hence, the effect of spalling is taken into account at cross-sectional level, however, in design, should the model be implemented, the damaged section would, by
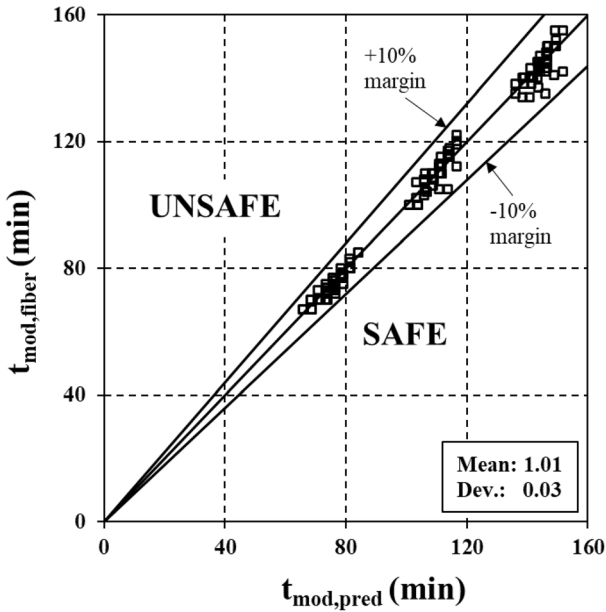
a) Corner spalling
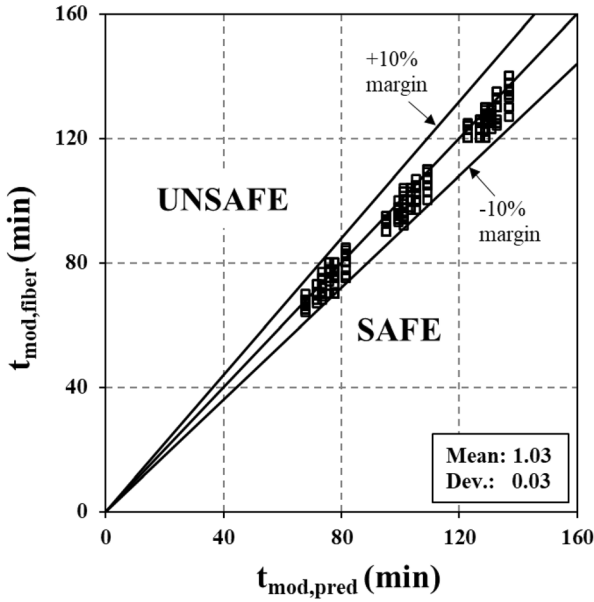
b) Surface spalling

Figure 18.   Modified Fire Resistance Times: Fiber Model Calculations vs. Proposal Predictions.

extension, be considered to be the same along the entire length of the column. Therefore, the model is erring on the side of caution and providing a conservative prediction that assumes the effect of the spalling in the whole element.

5. Concluding Remarks

In this work, a sectional model was used for evaluating the effect of spalling on the fire resistance of RC columns exposed to fire. The manifestation of spalling adopted in this work consisted of a loss of concrete cover and assumed that the reinforcing bar affected was directly exposed to the heat source after spalling. A parametric study was conducted to assess the influence of different parameters on the spalling effect and to compare the effects of surface and corner spalling. Finally, the results from the parametric study were used to build a proposal to calculate a modified fire resistance time for the effect of spalling in RC columns in situations in which the structural failure is not governed by buckling. As detailed above, some key assumptions were made, in absence of hard experimental evidence. Therefore, care should be taken if and when adopting the proposed design equations in actual projects. From this study, the next conclusions can be drawn:

- After spalling, the temperature of the directly exposed reinforcing bar increases much quicker than the temperature of those bars that are still protected by the concrete cover. Both the mechanical capacity and the temperature of the reinforcing bar affected by spalling are influenced by the spalling occurrence time. However, from 45 min on, the spalling initiation time has no remarkable effect.
- The consequent reduction in the concrete cover leaves the reinforcing steel directly exposed to the heat source, leading to a quick loss of resistance. The area of the cross-section affected is usually not large enough to influence the transmission of heat through the unspalled concrete of the cross-section.
- For a given load level and a required fire resistance time of a RC cross-section with spalling, it is possible to find the diagram of the same cross-section without spalling that is equivalent in the most critical quadrant.
- The negative effect of spalling on the RC cross-section resistance can be quantified by means of an additional fire exposure time, which ranges between 0 and 25 min for corner spalling and 0 and 35 min for surface spalling. In general, for required fire resistance times of 90 min or higher, the effect of surface spalling is more harmful. The exact value of this additional time depends on the column cross-section configuration, dimensions and load level.
- For higher values of concrete cover (40 mm) and required fire resistance times of 60 min, there is no difference in the effect of the two types of spalling. As the required fire resistance time increases and the concrete cover decreases, the difference augments.
- A conservative approach in design would be to consider exclusively surface spalling for RC columns with 8 reinforcing bars and fire resistance requirements equal or higher than 90 min. Contrarily, in RC columns with fire resistance

requirements lower than 90 min, both corner and surface spalling should be considered to evaluate which one is more damaging. For RC columns with 4 reinforcing bars, just corner spalling should be explicitly considered.

- The design equations developed, for surface and corner spalling, can predict the modified fire resistance time for the effect of spalling in RC columns with accuracy. These equations may be useful for practitioners to easily quantify the effect of spalling without an explicit modelling, considering the assumptions adopted in the model.

Acknowledgements

Declarations

Conflict of interest The authors declare that they have no known competing financial interests or personal relationships that could have appeared to influence the work reported in this paper.

Open Access

References

1. Dotreppe JC, Franssen JM, Vanderzeipen Y (1999) Calculation method for design of reinforced concrete columns under fire conditions. J Am Concr Inst 96(1):9–18
2. Khoury GA (2000) Effect of fire on concrete and concrete structures. Prog Struct Eng Mater 2:429–447
3. Deeny S, Stratford T, Dhakal RP, Moss PJ, Buchanan, AH (2008) Spalling of concrete: implications for structural performance in fire. 20th Australasian conference on mechanics of structure and materials
4. Gil AM, Fernandes B, Bolina FL, Tutikian BF (2018) Experimental analysis of the spalling phenomenon in precast reinforced concrete columns exposed to high temperatures. Rev IBRACON Estrut Mater 11(4):856–875
5. Jansson R (2013) Fire spalling of concrete—A historical overview. MATEC Web Conf 6(01001):1–11
6. Hertz KD (2003) Limits of spalling of fire-exposed concrete. Fire Saf J 38:103–116
7. Fib-International Federation for Structural Concrete (2007) Fib Bulletin 38: Fire design of concrete structures—materials, structures and modelling. Lausanne, Switzerland
8. Majorana CE, Salomoni VA, Mazzuccoa G, Khoury GA (2010) An approach for modelling concrete spalling in finite strains. Math Comput Simul 80:1694–1712
9. Lo Monte F, Gambarova PG (2015) Corner spalling and tension stiffening in heat-damaged R/C members: a preliminary investigation. Mater Struct 48:3657–3673
10. Miah MJ, Lo Monte F, Felicetti R, Carré H, Pimienta P, Borderie CL (2016) Fire spalling behaviour of concrete: role of mechanical loading (uniaxial and biaxial) and cement type. Key Eng Mater 711:549–555
11. Lo Monte F, Felicetti R, Meda A, Bortolussi A (2020) Explosive spalling in R/C structures exposed to fire: key aspects in experimental testing. Proc Ital Concr Days 42:372–384
12. Buch SH, Sharma UK (2019) Fire resistance of eccentrically loaded reinforced concrete columns. Fire Technol 55:1517–1552
13. Dwaikat MB, Kodur V (2009) Hydrothermal model for predicting fire-induced spalling in concrete structural systems. Fire Saf J 44(3):425–434
14. Lottman BBG, Koenders EAB, Blom CBM, Walraven JC (2013) Spalling of concrete due to fire exposure: a coupled fracture mechanics and pore pressure approach. MATEC Web Conf 6(05002):1–8
15. Peña DL, Albero V, Ibáñez C, Hospitaler A (2021) Sectional model for the fire evaluation of reinforced concrete columns subjected to biaxial bending. Eng Struct 247(113094):1–17
16. Wang L, Van Coile R, Caspeele R, Taerwe L (2017) Simplified method for evaluating the biaxial capacity of rectangular reinforced concrete columns during fire. Mater Struct 50:1–13
17. Kodur V, Raut N (2012) A simplified approach for predicting fire resistance of reinforced concrete columns under biaxial bending. Eng Struct 41:428–443
18. CEN-Comité Européen de Normalisation (2004) EN 1992-1-1 Eurocode 2: design of concrete structures, Part 1.1: general rules and rules for buildings. Brussels, Belgium
19. CEN-Comité Européen de Normalisation (2004) EN 1992-1-2 Eurocode 2: Design of concrete structures, Part 1.2: General rules–Structural fire design. Brussels, Belgium
20. MATLAB and Statistics Toolbox Release (2018) The MathWorks Inc. Natick, Massachusetts, United States
21. CEN-Comité Européen de Normalisation (2002) EN 1991-1-2 Eurocode 1: Actions on structures, Part 1.2: Actions on structures exposed to fire. Brussels, Belgium

22. Lie TT, Irwin RJ (1990) Evaluation of the fire resistance of reinforced concrete columns with rectangular cross- sections. Institute for Research in Construction, National Research Council of Canada, Ottawa, IRC Internal Report No. IRC-IR-601. https://doi.org/10.4224/20359214

23. Kodur V, Cheng F, Wang T, Latour J, Leroux P (2001) Fire resistance of high-performance concrete columns. Institute for Research in Construction, National Research Council of Canada, Ottawa, IRC Internal Report No. IRC-IR-834. https://doi.org/10.4224/20378506

24. Bresler B (1960) Design criteria for reinforced columns under axial load and biaxial bending. J Am Concr Inst 57(11):481–490

25. Ramamurthy L (1966) Investigation of the ultimate strength of square and rectangular columns under biaxially eccentric loads. J Am Concr Inst 13:263–298

26. Law A, Gillie M (2010) Interaction diagrams for ambient and heated concrete sections. Eng Struct 32(6):1641–1649